Low-wave-number statistics of randomly advected passive scalars

Alan R. Kerstein
Combustion Research Facility, Sandia National Laboratories, Livermore, California 94551-0969

Patrick A. McMurtry
Department of Mechanical Engineering, University of Utah, Salt Lake City, Utah 84112
(Received 21 April 1994)

A heuristic analysis of the decay of a passive scalar field, subject to statistically steady random advection, predicts two low-wave-number spectral scaling regimes analogous to the similarity states previously identified by Chasnov [Phys. Fluids **6**, 1036 (1994)]. Consequences of their predicted coexistence in a single flow are examined. The analysis is limited to the idealized case of narrow band advection. To complement the analysis, and to extend the predictions to physically more realistic advection processes, advection diffusion is simulated using a one-dimensional stochastic model. An experimental test of the predictions is proposed.

PACS number(s): 47.27.Gs, 05.40.+j, 02.50.−r

I. INTRODUCTION

Chasnov [1] recently performed a comprehensive study of the similarity states of passive scalar transport in decaying turbulence, complementing and in some respects clarifying previous work. Earlier work on this problem is summarized by Hinze [2]. Hinze notes that analogous questions for the case of statistically steady turbulence can likewise be posed, but are perhaps of less practical interest.

We propose that the statistically steady case is of interest for several reasons. First, there are physical manifestations of statistically steady turbulence that are of technological as well as fundamental interest. Examples include turbulence driven by buoyancy, free shear, and wall boundary layers. A particular example is considered in the latter portion of this paper, and experimentally testable predictions are obtained. Second, advection diffusion subject to statistically steady forcing is increasingly recognized as an important paradigm of turbulent mixing.

Many recent analytical and numerical studies of the steady-forcing case [3–8] involve the imposition of scalar boundary conditions that induce statistically steady scalar fluctuations. The main focus of these studies has been the interpretation of long-tailed scalar probability density functions (PDF's) observed experimentally [9–13]. In other studies of the steady-forcing case [6,14–16], decaying scalar fields are considered. Numerical simulations of this configuration typically involve domains of size comparable to the advection length scale, with periodic boundary conditions imposed. Again, the main focus has been the scalar PDF and related statistics, with reference to their evolution from a given initial state to an asymptotic similarity state.

The present focus is on low-wave-number spectral regimes of the scalar field, but results obtained here have some bearing on scalar PDF evolution. It is noted that the domain size relative to the advection length scale can affect the final similarity state. In particular, the low-wave-number dynamics of scalar decay in the limit of large domain size result in an asymptotically Gaussian PDF. Previously reported non-Gaussian asymptotic states of decaying scalar fields are manifestations of finite domain size. This observation does not detract from the validity or the physical relevance of the previous results because the finite-domain case is more common in physical applications than the case of an effectively infinite domain. The point is simply that some interesting non-Gaussian effects go away when very large domains are considered.

Low-wave-number properties of advection diffusion are studied here by heuristic analysis of the d-dimensional advection-diffusion equation, supported and extended by numerical simulations based on a one-dimensional stochastic model. The heuristic analysis, limited to the idealized case of narrow band advection, is presented in Sec. II. In Sec. III, it is shown that the linear-eddy model, a one-dimensional stochastic process used previously to investigate diverse properties of advection-diffusion processes [4,5,15,16], reproduces the predicted spectral scalings. On the basis of this result and mechanistic considerations, it is proposed that the linear-eddy model can plausibly be extended to cases of physical interest that are not amenable to heuristic analysis. Simulations of one such case are presented in Sec. IV. An experimental test of predicted behaviors is proposed in Sec. V.

II. NARROW BAND ADVECTION: ANALYSIS

Consider a scalar field $c(\mathbf{x},t)$ that evolves according to the d-dimensional advection-diffusion equation

$$\dot{c} + \mathbf{v}\cdot\nabla c = \kappa\nabla^2 c, \tag{1}$$

where κ is the molecular diffusivity and $\mathbf{v}(\mathbf{x},t)$ is a divergence-free, homogeneous, isotropic, statistically steady advection process. It is assumed that the power spectrum of $\mathbf{v}$ is concentrated in a narrow range about a characteristic wave number, the inverse of the advection length scale ξ_v.

More generally, a broad high-wave-number spectral tail is permitted, but not a low-wave-number tail. The latter restriction precludes the case of high-Reynolds-number Navier-Stokes turbulence, which develops spectral tails on both sides of the forcing wave number [17]. The postulated flow properties might correspond, e.g., to viscous flow with statistically steady mechanical forcing. The low-wave-number restriction is relaxed in computations discussed in Sec. IV.

It is likewise assumed that the low-wave-number content of the initial scalar field $c(\mathbf{x},0)$ is negligible. Computations discussed in Secs. III and IV involve spatially periodic $c(\mathbf{x},0)$.

The advection process is characterized by ξ_v and by a correlation time τ_v or, alternatively, by a velocity amplitude $v' \sim \xi_v/\tau_v$ and an effective diffusivity $\kappa_e \sim \xi_v^2/\tau_v$. Henceforth, length and time are scaled by ξ_v and τ_v, so v' and κ_e become nondimensional. Molecular-diffusive effects are parametrized by the Péclet number $\mathrm{Pe} = \kappa_e/\kappa$. Low-wave-number properties considered here are independent of Pe for $\mathrm{Pe} \gg 1$, reflecting the well-known irrelevance of molecular diffusion at length scales for which the characteristic molecular diffusion time greatly exceeds the characteristic advection time. In effect, scalar spectral intensity is transported in wave-number space by the advection process, with the dissipative action of molecular diffusion acting only at high wave numbers (corresponding to the "Batchelor scale" [17]).

Low-wave-number spectral properties of Eq. (1) are analyzed heuristically. Omitting numerical factors of order unity, the spatial Fourier transform of Eq. (1) is

$$\dot{a}(\mathbf{k}) - i\int a(\mathbf{k}')\mathbf{k}'\cdot\mathbf{b}(\mathbf{k}-\mathbf{k}')\,d^dk' = -\kappa k^2 a(\mathbf{k}), \quad (2)$$

where $a(\mathbf{k}) = \int c(\mathbf{x})\exp(i\mathbf{k}\cdot\mathbf{x})\,d^dx$ and $\mathbf{b}(\mathbf{k}) = \int \mathbf{v}(\mathbf{x})\exp(i\mathbf{k}\cdot\mathbf{x})\,d^dx$. Though not shown explicitly, a, $\mathbf{b}$, and c are functions of time t.

A small-$\mathbf{k}$ approximation is obtained by Taylor-expanding $\mathbf{b}(\mathbf{k}-\mathbf{k}')$ for small $\mathbf{k}$, namely, $\mathbf{b}(\mathbf{k}-\mathbf{k}') = \mathbf{b}(-\mathbf{k}') + (\mathbf{k}\cdot\nabla_{\mathbf{k}})\mathbf{b}(-\mathbf{k}') + \cdots$, where $\nabla_{\mathbf{k}}\mathbf{b}(-\mathbf{k}')$ is the $\mathbf{k}$-space gradient of $\mathbf{b}$ evaluated at $-\mathbf{k}'$.

For $\mathbf{k} = \mathbf{0}$, the integral in Eq. (2) reduces to the spatial integral of $\mathbf{v}\cdot\nabla c$, which is zero because c is conserved. To lowest nonvanishing order in $\mathbf{k} \ll 1$, Eq. (2) gives

$$\dot{a}(\mathbf{k}) - i\int a(\mathbf{k}')\mathbf{k}'\cdot(\mathbf{k}\cdot\nabla_{\mathbf{k}})\mathbf{b}(-\mathbf{k}')\,d^dk' = -\kappa k^2 a(\mathbf{k}). \quad (3)$$

Because κ does not affect low-wave-number properties for $\mathrm{Pe} \gg 1$, it suffices to consider the pure advection problem, corresponding to $\kappa = 0$. Henceforth, vector notation is dropped because only magnitudes of quantities are considered. With these simplifications, Eq. (3) is of the form $\dot{a}(k) = k\eta$, where η is a random process. This implies linear dependence of a on k for $k \ll 1$. The d-dimensional scalar spectrum scales with Fourier amplitude a according to $E_d(k) \sim k^{d-1}a^2(k)$, because $E_d(k)$ is obtained by integrating $|a^2(\mathbf{k})|$ over a $(d-1)$-dimensional shell in wave-number space [17]. Therefore $E_d(k) \sim g(t)k^{d+1}$ for low k, where $g(t)$ is a time-dependent coefficient.

Invoking narrow band advection, b is non-negligible only for k' of order unity, so η is proportional to $a(1)$. It is shown below that $a(1)$ decays as $t^{-(d+4)/4}$, causing the growth rate of $a(k)$, governed by $\dot{a}(k) = k\eta$, to decrease with time. Accordingly, $g(t)$ ceases to grow after an initial transient. Its maximum value is bounded as a consequence of the following property. Advection by a divergence-free flow conserves all single-point statistical properties of the scalar field, in particular the scalar variance c'^2. The relation $c'^2 \sim \int E_d(k)\,dk$ [usually taken to be an equality by choice of the normalization of $E_d(k)$ [2]] therefore implies a bound on the low-wave-number portion of $E_d(k)$.

In fact, this relation implies the eventual decay of the low-wave-number spectrum because the advection process transfers scalar variance to high wave numbers. The transfer mechanism is the cascade of scalar spectral intensity induced by the compressive-strain effect of the advection process. This mechanism underlies the classical k^{-1} scaling of $E_d(k)$ at wave numbers higher than the wave-number range of the advection process [17].

No rigorous procedure is known for analyzing this mechanism based on Eq. (1) or (2). Here a heuristic approach is adopted, based on the eddy-diffusivity picture [17]. It is postulated that the effect of the cascade on scalar evolution in the wave-number range $k < 1$ can be represented by replacing κ by κ_e in Eq. (1). The advective term on the left-hand side is retained to represent mechanisms other than the scalar cascade.

Therefore consider Eq. (3) with κ replaced by κ_e. Taking $a(k,t_0) \sim k$, where t_0 is the time at which the initial transient buildup of $a(k)$ is completed, this implies subsequent decay of the form $a(k,t) \sim k\exp(-\kappa_e k^2 t)$ and thus

$$E_d(k) \sim k^{d+1}\exp(-2\kappa_e k^2 t). \quad (4)$$

Integration of Eq. (4) over k gives $c'^2 \sim \hat{k}^{d+2} \sim t^{-(d+2)/2}$, where $\hat{k} = (\kappa_e t)^{-1/2}$. The exponential cutoff cannot extend to indefinitely high k, for if it did, c'^2 would vanish rather than remaining constant at large t. The $t^{-(d+2)/2}$ decay applies only to the contribution of wave numbers $k < \hat{k}$ to the scalar variance. Therefore consider $k > \hat{k}$.

The wave-number range $\hat{k} < k < 1$ is analyzed by first considering the time dependence of $a(1)$. The mechanism that generates scalar fluctuations at $k = 1$, not reflected in the development thus far, is the perturbation of low-wave-number scalar fluctuations by the advection process. In effect, low-wave-number scalar fluctuations play a role akin to an imposed scalar gradient. Accordingly, $a(1)$ is proportional to the gradient magnitude [18], i.e., the product of the characteristic amplitude c' of low-wave-number fluctuations (which decreases as $t^{-(d+2)/4}$,

as noted) and the characteristic wave number $\hat{k}$ (which decreases as $t^{-1/2}$). Therefore $a(1) \sim t^{-(d+4)/4}$, giving

$$E_d(1) \sim t^{-(d+4)/2}, \tag{5}$$

a slower time decay than indicated by Eq. (4).

The scalar spectrum for $\hat{k} < k < 1$ is analyzed by expressing Eq. (3) (again, with κ replaced by κ_e) in the form

$$\dot{a}(k) = -\kappa_e k^2 a(k) + k\eta, \tag{6}$$

where η is a noise of amplitude $a(1)$ and correlation time unity (in scaled units). Because $a(1)$ decays as a power of t, its characteristic time scale is the elapsed time t. Therefore the secular variation of η is slow enough so that a quasisteady picture can be adopted for the time regime $t \gg 1$. Namely, Eq. (6) is regarded as a linear Langevin equation [19], giving $a^2(k) \sim a^2(1)$, i.e., $a^2(k)$ independent of k. As earlier, $E_d(k) \sim k^{d-1}a^2(k)$, giving

$$E_d(k) \sim k^{d-1}t^{-(d+4)/2} \tag{7}$$

in this "equilibrium" wave-number range, so named because spectral amplitudes are determined by the balance of fluctuation and dissipation processes in Eq. (6).

The analysis motivates the following intuitive picture of the low-wave-number evolution of the power spectrum of a randomly advected scalar. Assuming a narrow band initial scalar spectrum, random advection induces a k^{d+1} low-wave-number spectral tail whose transient growth to a limiting amplitude occurs on the advection time scale τ_v. For given $k \ll 1/\xi_v$, subsequent exponential decay of the spectrum occurs on the time scale $\kappa_e^{-1}k^{-2}$ governing the cascade of scalar variance to higher wave numbers. Crossover to a regime of slower time decay is brought about by the direct transfer of scalar variance from low k to k of order $1/\xi_v$. This transferred scalar variance is fed back to low wave numbers, balancing the scalar cascade so as to establish a wave-number range with power-law time decay.

We note an analogy between the inferred spectral scalings Eqs. (4) and (7) and similarity states identified in Chasnov's [1] analysis of advection diffusion in three-dimensional decaying turbulence. In the low-wave-number limit, Chasnov obtained $E_3(k) \sim k^4$ for a spatially homogeneous scalar field and $E_3(k) \sim k^2$ for the case of an imposed scalar gradient. The powers of k correspond to those of Eqs. (4) and (7), respectively, for $d = 3$. Moreover, a mechanistic connection can be identified.

The initial transient buildup of $a(k)$ leading to the power-law scaling in Eq. (4) is governed by a time scale t_0 that corresponds to the advection time scale τ_v. The decay of turbulence is governed by the same time scale, so the transient buildup in decaying turbulence differs from the case analyzed here only by an order-unity factor reflecting the decay of turbulence intensity over the time interval t_0. Therefore, the initial development of the scaling in Eq. (4) is not fundamentally affected by the occurrence or nonoccurrence of turbulence decay.

As reflected by the nomenclature we have adopted, the wave-number range governed by Eq. (7) equilibrates on a faster time scale than the wave-number range governed by k^{d+1} scaling. In effect, the latter range is a low-wave-number reservoir of scalar variance. This reservoir acts as an imposed scalar gradient driving the scalar fluctuations at higher wave numbers. Hence we have the mechanistic equivalence to the imposed-gradient configuration analyzed by Chasnov.

The distinct feature in the present situation is the slow transient induced by statistically steady advection, reflected by the time-dependent term in Eq. (4) and the consequent time dependence of Eq. (7). Curiously, maintenance of the advection induces transient scalar decay, while decay of advection leads, as Chasnov shows, to an invariant final state of the scalar. The scalar decay in the present situation leads to the coexistence of two low-wave-number scaling regimes in a single configuration.

III. NARROW BAND ADVECTION: STOCHASTIC SIMULATION

The heuristic analysis presented here does not establish the picture inferred in Sec. II as the uniquely plausible low-wave-number scenario. We seek further support for this picture by performing numerical simulations of advection diffusion.

Multidimensional numerical simulations with sufficient dynamic range to resolve the advection process and capture the low-wave-number scalings would be very costly. Here the linear-eddy model is used to simulate stochastic advection in one spatial dimension. The simulation method, described in detail elsewhere [4,5], involves deterministic numerical solution of the diffusion equation $\frac{\partial c}{\partial t} = \kappa \frac{\partial^2 c}{\partial x^2}$ on a linear domain, punctuated by a random sequence of instantaneous events that advect the scalar field. Each event involves spatial rearrangement of a randomly selected interval of the domain. Two alternative rearrangement rules, "inversion" (a spatial flip) and the "triplet map" (a one-dimensional analog of the baker's map) are employed. (These rules are measure preserving, i.e., they maintain the same scalar conservation laws as divergence-free flow.) The interval size either is fixed or is randomly selected for each event based on a specified size-versus-frequency distribution. The initial scalar field is periodic, with either sinusoidal or telegraphic spatial dependence. Low-wave-number properties are found to be insensitive to these and other variations.

As illustrated in Fig. 1, computed spectra highlight the remarkable mechanistic intricacy of low-wave-number scalar evolution. In Fig. 2, spectra for the illustrative case are plotted in rescaled coordinates to demonstrate their collapse with respect to the scalings derived in Sec. II.

Unlike low-wave-number properties, high-wave-number properties are sensitive to details of the advection process. For example, the oscillations seen at high k are specific to the rearrangement rule employed in the computation. The triplet map involves threefold compression of the scalar field in a randomly selected interval, re-

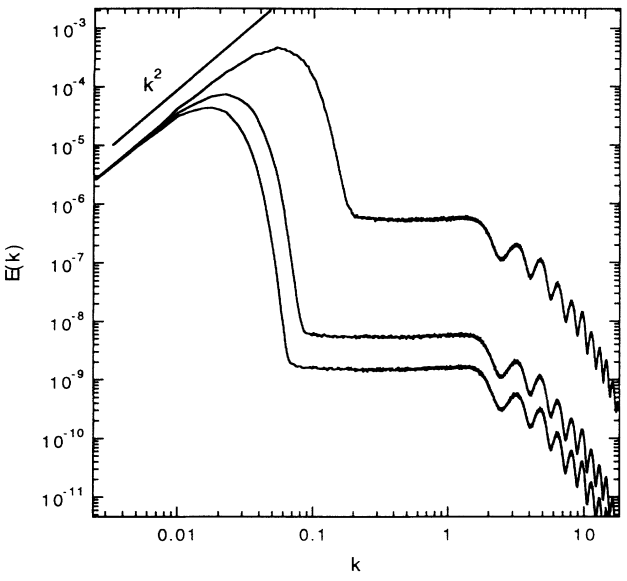

FIG. 1. Time evolution of the scalar power spectrum $E(k)$ obtained by linear-eddy simulation using the triplet-map rearrangement rule with fixed interval size $L = 2\pi$, corresponding to wave number $k = 2\pi/L = 1$. For the case shown, Pe=210 and the initial scalar field is sinusoidal with period 2π and scalar variance $\frac{1}{2}$. Curves (top to bottom) correspond to $t = 5.77$, 28.8, and 57.7. Here t is expressed in units of L^2/κ_e, where κ_e is the effective diffusivity of the advection process. A line segment of slope k^2 indicates the low-wave-number scaling.

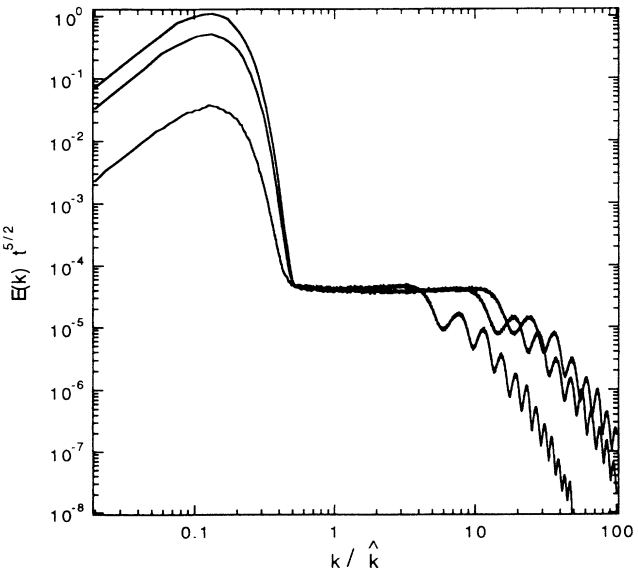

FIG. 2. Spectra of Fig. 1, replotted as $t^{5/2}E(k)$ versus $k/\hat{k}$ to demonstrate the time scalings of the equilibrium range amplitude, given by Eq. (4), and the low-wave-number cutoff $\hat{k} = t^{-1/2}$ (based on the time units of Fig. 1).

placement of the scalar field within the interval by three copies of the compressed image, and inversion of the central image. (See Ref. [4] for an illustration.) Because the first and last images are identical, the spatial autocorrelation exhibits a bump at their separation, $\frac{2}{3}$ of the interval size, resulting in oscillatory modulation of the power spectrum. Other rearrangement rules not subject to this artifact yield smooth spectra.

Model-specific high-k properties do not impact the underlying scalings at low or high k. For example, the high-k spectrum for the case of Figs. 1 and 2 but with Pe=21 000 (not shown) likewise oscillates, but the envelope of the oscillations exhibits the k^{-1} scaling governing the viscous-convective regime [17], which extends in this instance from $k = 1$ to the Batchelor wave number. (The k^{-1} scaling is not seen in Fig. 1 due to the limited wave-number range of the viscous-convective regime for this case.) Though the model represents advection as an event sequence rather than a continuum flow, the compression mechanism embodied in the triplet map can be viewed as a mechanistically valid analog of fluid-mechanical compressive strain. The extent and limits of validity of this analogy are considered in detail elsewhere [4].

As an aside, it is noted that the scalar PDF during the decay period is consistently found to be Gaussian. A decaying scalar field subject to statistically steady random advection exhibits Gaussian statistics because the dominant fluctuations at large t are at low wave numbers and therefore are the result of many independent motions in a spatial domain that is large compared to the advection length scale. PDF's obtained by high-pass filtering the simulated scalar field are found to be long tailed. This is because the high-pass-filtered scalar field is effectively subject to an imposed scalar gradient corresponding to the dominant low-wave-number modes. It has been shown that the linear-eddy model yields long-tailed scalar PDF's for the imposed-scalar-gradient configuration [4,5]. The mechanism is somewhat different from the mechanism responsible for long-tailed scalar PDF's in continuum flow subject to an imposed scalar gradient [8]. A recently proposed general classification of PDF shapes for diverse nonequilibrium statistical processes provides a framework for interpreting these observations [20].

IV. TURBULENT ADVECTION

The assumption that advection is a narrow band process is unrealistic because momentum is subject to transport processes analogous to those transporting the scalar. Consequently, the flow field tends to develop a low-wave-number spectral tail by much the same mechanism as for the passive scalar. Indeed, studies of this low-wave-number flow property predate the study of the analogous scalar property; k^4 low-wave-number scaling of the turbulence energy spectrum is well known [17].

If a k^{d+1} low-wave-number tail of the energy spectrum is assumed in the analysis of Sec. II, the simplifications that render the analysis tractable are no longer valid. We use the linear-eddy model to investigate this case. Though the validity of the model for this purpose is not

conclusively established, the agreement of the linear-eddy simulations of Sec. III with the analytical predictions of Sec. II indicates that the low-wave-number properties of the model are at least plausible.

A given energy spectrum is emulated within the model by a suitable choice of the size-versus-frequency distribution $f(l)$ of mapping intervals. It has been shown [4] that the choice $f(l) \sim l^{-q}$ leads to an advection process whose effective diffusivity ("eddy diffusivity") as a function of "eddy size" l is $\kappa_l \sim l^{4-q}$. In particular, $q = \frac{8}{3}$ corresponds to the inertial-range scaling $\kappa_l \sim l^{4/3}$. Inertial-range properties of a scalar advected according to this prescription have been verified [4].

More generally, the usual dimensional analysis [17] gives $\kappa_l \sim [lE(l)]^{1/2}$, where $E(l)$ denotes the turbulence energy spectrum parametrized by $l = 1/k$. The choice $E(l) \sim l^{-(d+1)}$, corresponding to the case of interest here, gives $\kappa_l \sim l^{-d/2}$, and thus $q = (8+d)/2$.

Ostensibly, the dimensionality of realistic flows is $d = 3$. However, there is an important case for which the appropriate choice is $d = 1$. That case is fully developed turbulent pipe flow. Though the flow is three dimensional at the scale of the pipe diameter, there is only one direction along which flow or scalar fluctuations of size much greater than this can develop. Therefore, pipe flow is effectively one dimensional with respect to its low-wave-number properties.

To simulate the decay of scalar fluctuations in turbulent pipe flow, we therefore take $d = 1$. The functional form of $f(l)$ used in the simulations is $f(l) = \lambda(l/l_0)^{-9/2}$ for $l > l_0$, where l_0 is an eddy-size cutoff. (The frequency factor λ is subsumed in the effective diffusivity κ_e characterizing the advection process; see Ref. [4].) The relation $L^2 \equiv \int l^3 f(l)\,dl / \int l f(l)\,dl = 5l_0^2$ determines a characteristic length scale L for this eddy distribution [21]. This length scale is used to normalize plotted results.

This $f(l)$ is not a quantitatively accurate representation of the eddy distribution for all l. Simulations using this $f(l)$ are intended to identify the qualitative effects of a long-tailed eddy distribution, as may occur in turbulent pipe flow, on the asymptotic scalings of the low-wave-number scalar statistics. Figures 3 and 4 show spectra obtained using this $f(l)$, but with the model formulation and parameter assignments chosen to be equivalent in all other respects to the case plotted in Figs. 1 and 2.

The plots indicate that some but not all of the narrow band results generalize to the pipe-flow case. Equation (4) and the time dependence of Eq. (7) remain valid, but the wave-number dependence of Eq. (7) no longer applies. The imperfect collapse of the scaled spectra for $t = 5$ and 10 indicates slow convergence to asymptotic scalings; see Sec. V for further discussion.

This outcome reflects the following considerations. The low-wave-number k^2 regime develops in a time of order τ_v, where τ_v is now the time scale of the small-l ($l \approx l_0$) events. The large-l events are irrelevant on this time scale, so they do not affect the k^2 scaling. Eddy-diffusivity effects are likewise small-l dominated because $\kappa_l \sim l^{4-q} \sim l^{-1/2}$. Therefore the diffusive cutoff in Eq. (4) is unaffected. Eddy diffusivity governs the rate of decay of the scalar-variance reservoir feeding the equilib-

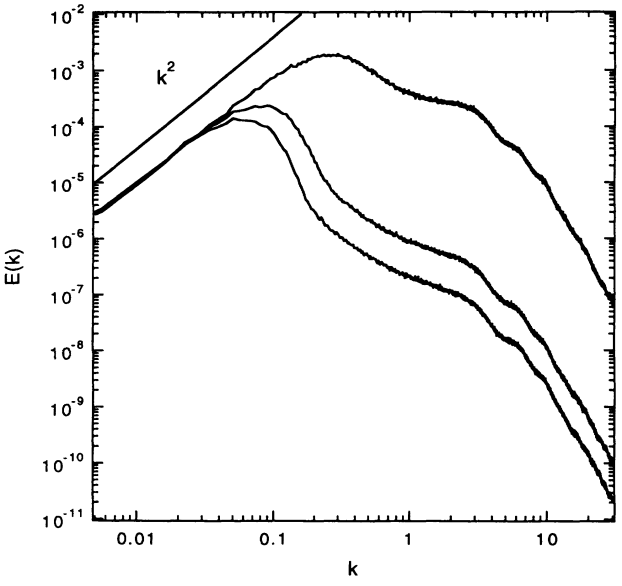

FIG. 3. Time evolution of the scalar power spectrum $E(k)$ obtained by linear-eddy simulation using the triplet-map rearrangement rule with a power-law distribution of interval sizes l, as specified in the text. The characteristic length scale L of this distribution is set equal to 2π, corresponding to wave number $k = 2\pi/L = 1$. As in the case plotted in Fig. 1, Pe=210 and the initial scalar field is sinusoidal. The period is $2\pi l_0/L$, where $l_0 = L/\sqrt{5}$ is the lower bound of the interval-size distribution, and the initial scalar variance is $\frac{1}{2}$. Curves (top to bottom) correspond to $t = 1$, 5, and 10 (in units of L^2/κ_e). A line segment of slope k^2 indicates the low-wave-number scaling.

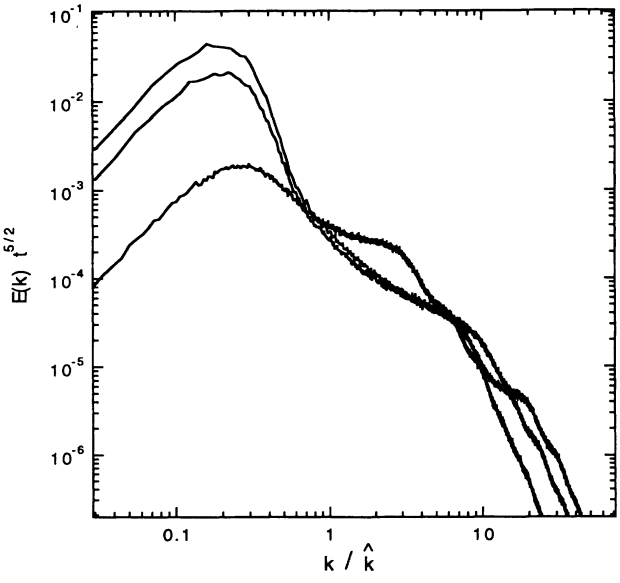

FIG. 4. Spectra of Fig. 3, replotted in the format of Fig. 2.

rium regime, so the time decay of the level of the equilibrium spectrum obeys the same scaling as the narrow band case. The dynamics within the equilibrium range are not intrinsically dominated by small eddies, so it is plausible that the k dependence in Eq. (7) no longer applies.

We do not attempt to interpret the linear-eddy result for the k dependence in the equilibrium range for the pipe-flow case. We view it as a model prediction whose validity may be tested by means of a laboratory experiment.

V. IMPLICATIONS FOR PIPE-FLOW MIXING

With regard to experimentation, it is of interest to compare the results of Sec. IV to present-day understanding of turbulent-pipe-flow mixing. In their classic paper that verified the viscous-convective scalar spectral subrange predicted by Batchelor [22], Nye and Brodkey [23] examined large-scale mixing properties in turbulent pipe flow by measuring the axial decay of a quantity that, for present purposes, is equivalent to scalar variance. Adopting a plug-flow picture of pipe flow, they interpreted the axial decay in terms of Corrsin's [24] theory of the time decay of scalar variance in a stirred tank. In this formulation, scalar and advection length scales are limited by a fixed upper bound, leading (by dimensional analysis) to exponential decay of scalar fluctuations. The measurements by Nye and Brodkey suggest exponential decay at a rate consistent with a length-scale bound on the order of the pipe diameter. However, the axial range of their measurements was not very large, and they found several indications that initial transients had not fully relaxed.

The analysis of the narrow band case in Sec. II predicts $t^{-(d+2)/2}$ decay of the low-wave-number contribution to scalar variance. That analysis omits molecular diffusion effects, which are significant only at high wave numbers. In the absence of molecular diffusion, the total scalar variance is constant. The effect of nonzero molecular diffusivity, however small, is to dissipate scalar variance cascading to high wave numbers, causing the total scalar variance to be dominated by the low-wave-number contribution [1]. Therefore the analysis implies $t^{-(d+2)/2}$ decay of the total scalar variance for large but finite Pe.

Scalar-variance time histories obtained from the linear-eddy simulations discussed in Secs. III and IV are plotted in Fig. 5. For the narrow band case, the $t^{-3/2}$ decay predicted for $d = 1$ is obtained. For the case that emulates the pipe-flow configuration, the large-t asymptote is approached gradually [25]. The plot indicates t^{-2} decay for $t > 3$. The mechanistic considerations of Sec. IV suggest eventual relaxation to $t^{-3/2}$ decay.

The physical mechanism underlying this slower-than-exponential decay is the initial transfer of scalar spectral intensity to low wave numbers, creating a reservoir of large-scale fluctuations that are then slowly consumed by the eddy-diffusion mechanism. In the pipe-flow context, this picture indicates the essential role of fluctuations on length scales much larger than the pipe diameter. Thus we propose that the plug-flow picture of turbulent pipe flow (i.e., the representation of the pipe flow as a stirred tank moving axially at the mean flow velocity) omits the rate-limiting factor determining the far-field decay of scalar variance.

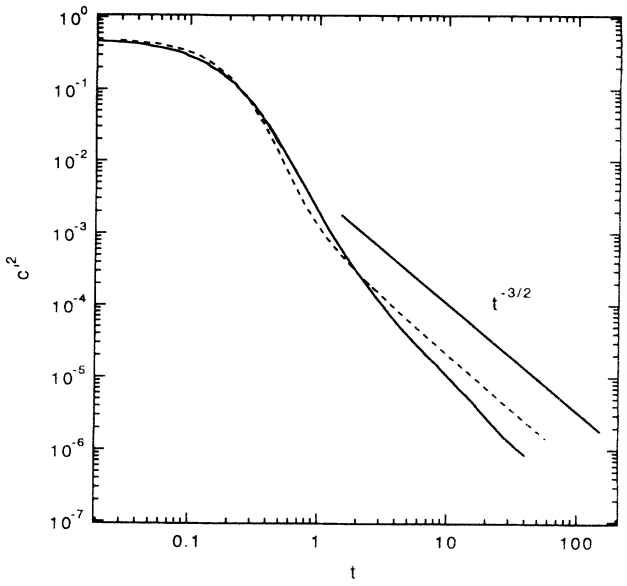

FIG. 5. Scalar variance c'^2 versus time t from the linear-eddy simulations corresponding to Fig. 1 (dashed) and Fig. 3 (solid), with time scaled as in those figures. A line segment of slope $t^{-3/2}$ indicates the predicted asymptotic scaling.

It would be interesting to redo the Nye and Brodkey experiment with technologies now available to measure scalar concentrations over a much wider dynamic range than was possible in the original experiment. This would permit measurements far enough downstream to obtain a definitive test of the present predictions versus the Corrsin theory. The spectral scalings as well as the variance decay law should be testable. Because the low-wave-number components of the scalar field determine both properties, high spatial resolution is not required. This should be helpful in obtaining a signal-to-noise ratio sufficient to detect small-amplitude concentration fluctuations.

ACKNOWLEDGMENTS

This research was supported by the Division of Engineering and Geosciences, Office of Basic Energy Sciences, U.S. Department of Energy, and by the National Science Foundation under Grant No. CTS9258445.

[1] J. R. Chasnov, Phys. Fluids **6**, 1036 (1994).
[2] J. O. Hinze, *Turbulence*, 2nd ed. (McGraw-Hill, New York, 1975).
[3] A. Pumir, B. I. Shraiman, and E. D. Siggia, Phys. Rev. Lett. **66**, 2984 (1991).
[4] A. R. Kerstein, J. Fluid Mech. **231**, 261 (1991).
[5] M. Holzer and A. Pumir, Phys. Rev. E **47**, 202 (1993).
[6] A. J. Majda, Phys. Fluids A **5**, 1963 (1993).

[7] S. L. Christie and J. A. Domaradzki, Phys. Fluids A **5**, 412 (1993).
[8] B. I. Shraiman and E. D. Siggia, Phys. Rev. E **49**, 2912 (1994).
[9] B. Castaing, G. Gunaratne, F. Heslot, L. Kadanoff, A. Libchaber, S. Thomae, X.-Z. Wu, S. Zaleski, and G. Zanetti, J. Fluid Mech. **204**, 1 (1989).
[10] M. Sano, X.-Z. Wu, and A. Libchaber, Phys. Rev. A **40**, 6421 (1989).
[11] Jayesh and Z. Warhaft, Phys. Rev. Lett. **67**, 3503 (1991).
[12] Jayesh and Z. Warhaft, Phys. Fluids A **4**, 2292 (1991).
[13] J. Gollub, J. Clarke, M. Gharib, B. Lane, and O. Mesquita, Phys. Rev. Lett. **67**, 3507 (1991).
[14] V. Eswaran and S. B. Pope, Phys. Fluids **31**, 506 (1988).
[15] P. A. McMurtry, T. C. Gansauge, A. R. Kerstein, and S. K. Krueger, Phys. Fluids A **5**, 1023 (1993).
[16] M. A. Cremer, P. A. McMurtry, and A. R. Kerstein, Phys. Fluids **6**, 2143 (1994).
[17] M. Lesieur, *Turbulence in Fluids*, 2nd ed. (Kluwer, Dordrecht, 1990).
[18] This follows from dimensional considerations, but can also be inferred from Eq. (2). Due to the dissipative cutoff of a, the dominant contribution to the integral in Eq. (2) is from small k'. For $k = 1$, the argument of $\mathbf{b}$ is insensitive to $k' \ll 1$, so $\mathbf{b}$ can be removed from the integral. The integral is then of order $|\nabla c|$ evaluated at a particular value of x. The linear dependence of $a(1)$ on the scalar gradient follows because Eq. (2) is linear in a. It should be noted that substitution of $a(k', t) \sim k' \exp(-\kappa_e k'^2 t)$ into the integrand is not appropriate because this scaling estimate neglects phase dependences that affect the value of the integral.
[19] For the Langevin equation $\dot{u} = -\beta u + \eta$, where η is a noise with amplitude A and correlation time τ, the steady-state fluctuation intensity obeys $\langle u^2 \rangle \sim A^2/(\beta\tau)$. See S. Chandrasekhar, Rev. Mod. Phys. **15**, 1 (1943).
[20] J. M. Deutsch, Phys Rev. E **48**, R4179 (1993).
[21] L is defined so that an advection process with the same eddy frequency, but with fixed interval size L for all mapping events, would have the same κ_e as for the stated distribution of interval sizes. See Ref. [4].
[22] G. K. Batchelor, J. Fluid Mech. **5**, 113 (1959).
[23] J. O. Nye and R. S. Brodkey, J. Fluid Mech. **29**, 151 (1967).
[24] S. Corrsin, AIChE J. **10**, 870 (1964).
[25] The slow relaxation for this case can be understood as follows. The eddy-diffusivity picture of variance decay is valid provided that the characteristic eddy size is much smaller than the length scale of the fluctuations being dissipated. That length scale is $1/\hat{k} \sim (\kappa_e t)^{1/2}$. Based on Sec. IV, the contribution of size-l eddies to κ_e is of order $(l/L)^{-1/2}$. The contribution of size-$(1/\hat{k})$ eddies to κ_e is therefore of order $(\hat{k}L)^{1/2} \sim (\kappa_e t/L^2)^{-1/4}$. Validity of the eddy-diffusivity analysis therefore requires $(\kappa_e t/L^2)^{-1/4} \ll 1$, indicating that the onset of asymptotic behavior may not occur until t is extremely large. In this regard, note that the collapse of the scaled spectra is not as precise in Fig. 4 as in Fig. 2.